Research Paper

A significant risk factor for poststroke depression: the depression-related subnetwork

Songran Yang, PhD*; Ping Hua, PhD*; Xinyuan Shang, MM; Zaixu Cui, MM; Suyu Zhong, MM; Gaolang Gong, PhD; Glyn W. Humphreys, PhD

Background: Despite being one of the direct causes of depression, whether stroke-induced neuroanatomical deterioration actually plays an important role in the onset of poststroke depression (PSD) is controversial. We assessed the structural basis of PSD, particularly with regard to white matter connectivity. **Methods**: We evaluated lesion index, fractional anisotropy (FA) reduction and brain structural networks and then analyzed whole brain voxel-based lesions and FA maps. To understand brain damage in the context of brain connectivity, we used a graph theoretical approach. We selected nodes whose degree correlated with the Hamilton Rating Scale for Depression score ($p <$ 0.05, false discovery rate–corrected), after controlling for age, sex, years of education, lesion size, Mini Mental State Examination score and National Institutes of Health Stroke Scale score. We used Poisson regression with robust standard errors to assess the contribution of the identified network toward poststroke major depression. **Results:** We included 116 stroke patients in the study. Fourteen patients (12.1%) had diagnoses of major depression and 26 (22.4%) had mild depression. We found that lesions in the right insular cortex, left putamen and right superior longitudinal fasciculus as well as FA reductions in broader areas were all associated with major depression. Seventeen nodes were selected to build the depression-related subnetwork. Decreased local efficiency of the subnetwork was a significant risk factor for poststroke major depression (relative risk 0.84, 95% confidence interval 0.72–0.98, $p = 0.027$). **Limitations:** The inability of DTI tractography to process fibre crossings may have resulted in inaccurate construction of white matter networks and affected statistical findings. **Conclusion:** The present study provides, to our knowledge, the first graph theoretical analysis of white matter networks linked to poststroke major depression. These findings provide new insights into the neuroanatomical substrates of depression that develops after stroke.

Introduction

Poststroke depression (PSD) is one of the most common emotional disorders afflicting those who experience stroke. A meta-analysis has indicated that the prevalence of major or mild depression is approximately 18% (range 8%–46%),[1] with the presence of PSD being associated with increased mortality.[2] Converging evidence has implicated particular neural networks in the pathophysiology of mood disorders.[3] However, despite being one of the direct causes of depression, whether stroke-induced neuroanatomical deterioration actually plays an important role in the onset of PSD is still controversial. Previous neuroimaging studies have focused mainly on regional differences and severity of local brain lesions.[4] In addition, an often-cited meta-analysis that reported no clear association between PSD and any specific lesion location or hemisphere[4] has fueled intense debate. Recently, although statistical parametric mapping linked affective depression to lesions centred in the left basal ganglia and left frontal cortex, the conclusions remain in doubt because results were not corrected for multiple comparisons.[5,6]

Diffusion tensor imaging (DTI) is a noninvasive technique that assesses white matter connectivity, particularly fibre density and myelination. In addition, structural brain network interactions can be quantified using brain graphs[7,8] in which neuroanatomical regions are defined as a set of nodes and DTI-derived white matter connections act as interconnecting edges.[7] Using this approach, a disruption of neural topology has been shown in several brain diseases,[9–11] including those occurring in chronic stroke patients.[12]

Here, we evaluated 3 markers of brain-damage severity: lesion index, fractional anisotropy (FA) reduction and brain structural networks. We hypothesized that a specific brain subnetwork is associated with PSD and that the damage to it might serve as a predictor of poststroke major depression. We constructed a depression-related subnetwork based on

data from 116 stroke patients, and we preliminarily assessed the unique contribution of the identified subnetwork for the presence of poststroke major depression.

Methods

Participants

Participants were ischemic stroke patients admitted to Guangzhou First People's Hospital between January 2012 and December 2013. Patients were included if they met the following 5 criteria. First, they were required to have a National Institutes of Health Stroke Scale (NIHSS) score of 6 or lower. Second, patients had to be conscious, able to cooperate with the interview and provide informed consent and complete the scale evaluations and a clinical interview for diagnosis of depression; those with severe aphasia who could not satisfy this criterion were excluded. Third, patients had to undergo a series of brain MRI scans, including T_1, T_2, fluid-attenuated inversion-recovery (FLAIR) and DTI, within 7 days of stroke onset, and these scans had to be of good quality and available for analysis. Fourth, the clinical interview was required to confirm that the patients had no history of schizophrenia, major depression, anxiety, dementia, drug abuse, antidepressant use at stroke onset, or a family history of mental disorders. Finally, we enrolled patients only if they were not severe drinkers (> 42 drinks/wk, where 1 drink equalled 8 g of alcohol);[13] severe drinkers were excluded because chronic high-level alcohol intake has been linked to grey matter shrinkage and white matter degradation.[14] We also classified other alcohol-intake levels for later analyses (nondrinkers: no drinking or < 1 drink/wk; light drinkers: 1–15 drinks/wk; moderate drinkers: 16–42 drinks/wk; ex-drinkers: currently no drinks/wk[15]).

An experienced neuropsychologist performed the clinical interview to diagnose depression within 1 month after stroke onset according to DSM-IV criteria. The severity of depression was assessed using the 24-item Hamilton Rating Scale for Depression (HAMD-24)[16] within 1 month after stroke onset. To be included in the major depression group in our final analysis, participants had to meet DSM-IV criteria for major depressive disorder and score at least 20 on the HAMD.[1] The other participants were assigned to either the control group or a mild depression group according to the HAMD cut-off point of 10.

The NIHSS scores were recorded at the time of admission to the hospital. One month after stroke onset, we obtained scores on the Mini Mental State Examination (MMSE) and the Barthel Index.

A comprehensive document elaborated on the purpose of the study and the intended uses of the data. Participants (and their surrogates) reviewed the document and the consent form. In cases when the patient had visual neglect or other reading problems, the researcher explained the documents in detail. The participants who agreed to participate gave their informed consent, with the forms being signed by the patients themselves or by their surrogates. The Ethics Committee of Guangzhou First People's Hospital approved the research protocol.

Imaging data acquisition

We acquired MRI scans using a Siemens Verio 3.0 T scanner. Restraining foam pads were used to minimize head motion. We scanned the T_1-weighted images in the sagittal plane with the following parameters: repetition time (TR) 1900 ms, echo time (TE) 3.44 ms, inversion time (TI) 900 ms, flip angle 9°, voxel size $1 \times 1 \times 1$ mm³. The FLAIR T_2 images were scanned on the axial plane with a slice thickness of 5 mm. We used a single-shot echo-planar imaging (EPI) sequence to acquire DTI data, with coverage of the whole brain. Each scan consisted of 30 diffusion-weighted directions with a b value of 1000 s/mm² and 1 additional volume without diffusion weighting (b0 image) with the following parameters: TR 8000 ms; TE 89 ms; slice thickness 3 mm, no gap; field of view 240×240 mm; acquisition matrix 128×128; and 2.2×2.2 mm in-plane resolution.

Imaging data preprocessing

We included a lesion index and an FA value to reflect the severity of brain damage for each voxel. Specifically, each voxel from each patient had a dichotomous lesion value, reflecting a given voxel as being lesioned or intact, and a continuous FA value, providing information for white matter connectivity. We then analyzed the whole brain voxel-based lesion and FA map.

Structural MRI data

For the 3-dimensional imaging data, we first coregistered each of the 2 structural sequences on individual space with 6 degrees of freedom using the FMRIB Linear Image Registration Tool.[17] An experienced radiologist (X.S.) manually drew each patient's lesion contour slice by slice, visually referring to the FLAIR T_2 images. Each patient's structural images were registered into Montreal Neurological Institute (MNI) standard space and resliced into $1 \times 1 \times 1$ mm³ voxels using a nonlinear registration method. The lesion description was also transformed into MNI space.

Whole brain statistical parametric mapping

We used the registered lesion regions to analyze the association between stroke lesions and the severity of depression. Three contrasts (mild depression – control v. major depression – control v. major depression – mild depression) were used to test for significant differences in lesion. Voxel × voxel t tests were applied in standard brain coordinates using Statistical Parametric Mapping 8 (SPM8, Wellcome Department of Cognitive Neurology). Because they have been linked to depression in previous studies,[18,19] we included age, sex, years of education, lesion size, MMSE score and NIHSS score as covariates to control for confounding factors. We considered results to be significant at $p < 0.05$, family-wise error (FWE)–corrected, with a cluster size > 100.

Diffusion tensor imaging data

We extracted the FA map of each patient in 3 steps: BET, which involves skull removal; eddycorrect, which involves

correction of eddy current distortion; and DTIFIT, which involves building diffusion tensor models. We then registered the FA maps with the FMRIB FA template in standard MNI space using nonlinear registration.

Whole brain voxel-based FA analysis

We conducted voxel-based analysis of FA using SPM8. All FA maps were smoothed using a Gaussian kernel ($\sigma = 1$). We performed a *t* test for smoothed FA values using the same 3 contrasts listed above and again included age, sex, years of education, lesion size, MMSE score and NIHSS score as covariates. We identified brain regions that showed lower FA values in the 3 contrasts. We set thresholds at $p <$ 0.05, FWE-corrected, with a cluster size > 100.

Fractional anisotropy values in intact areas of lesioned tracts

We identified 20 major white matter tracts according to the Johns Hopkins University white matter tractography atlas (25% threshold subtemplate).[20] To evaluate whether FA values revealed information secondary to the infarct, we obtained the mean FA for 17 tracts by averaging the FA values of all intact voxels in each tract and compared them with cases that did or didn't have lesions in that tract. The remaining 3 tracts (bilateral cingulum hippocampus and major forceps) were not analyzed because they were lesioned in fewer than 10 participants. To evaluate whether light to moderate alcohol intake affected FA values, we compared the mean FA values of all intact voxels in the 17 identified white matter tracts between nondrinkers and light to moderate drinkers.

Brain subnetworks correlated with PSD

To identify whether deterioration in brain network interactions plays an important role in the occurrence of PSD, we applied DTI tractography to construct white matter networks within the brain and used graph analyses to quantify the topological properties of the constructed networks.

Construction of brain white matter networks using DTI tractography

We constructed the white matter matrix using the pipeline software PANDA.[21,22] The automated anatomic labelling (AAL) atlas[23] (90 regions, excluding the pons and cerebellum) was used to define the nodes of the white matter network. We defined edges by applying deterministic fibre tracking[24] using the continuous tracking method of fibre assignment.[25] All possible fibres within the brain were first reconstructed by seeding from voxels with an FA value greater than 0.2. For every pair of brain nodes/regions, fibres with end points located in their respective masks were considered to be the ones linking the 2 nodes. Following standard practice,[26,27] we defined the averaged FA of the linking fibres as the strength for each connection. For each individual, we generated a network matrix in which each row/column represented a brain node/region and each element represented the averaged FA of the linking fibres between nodes.

We investigated the topological properties of brain networks at both global and nodal levels using the GRETNA toolbox.[28] The degree for each of the nodes was quantified[29–31] and used here as a reliable index of regional connectivity. The small-world coefficient σ was used to evaluate small-world behaviour.[32] For the whole brain network, we also calculated local and global efficiency. The definitions of these topological parameters were as follows.

(a) The nodal degree was defined as[29]

$$K_i = \sum_j a_{ij}$$

where a_{ij} indicates the number of edges between node i and node j.

(b) The small-world coefficient (σ) was defined as[33]

$$\sigma = \frac{C / C_{rand}}{L / L_{rand}}$$

where the numerator indicates the clustering coefficient of the real network compared with an equivalent random network, and the denominator represents the path length of the real network compared with the equivalent random network. A $\sigma > 1$ indicates small-world behaviour.

(c) Network global efficiency was defined as[29]

$$E_{glob} = \frac{1}{N(N-1)} \sum_{i,j \in V, i \neq j} \frac{1}{l_{ij}}$$

where l_{ij} represents the shortest path length between node i and node j, and N denotes the number of nodes in the network. Global efficiency represents how well the information is transferred within a network, at a global scale.

(d) Network local efficiency was calculated as[29]

$$E_{loc}(G) = \frac{1}{N} \sum_{i \in G} E_{glob}(G_i)$$

where G_i represents the subgraph composed from the nearest neighbours of node i. Local efficiency represents how much the complex network is fault tolerant and indicates how well the information is communicated within the neighbours of a given node when this node is removed.

Subdivision of the whole brain network

We correlated each nodal degree with the HAMD-24 score across participants, controlling for age, sex, years of education, lesion size, MMSE score and NIHSS score, and used the false-discovery rate (FDR) method to correct for multiple comparisons ($p < 0.0024$, corrected $p < 0.05$). We selected those nodes whose degree was correlated to the HAMD-24 scores to construct a depression-related subnetwork. The

other nodes constituted a subnetwork unrelated to depression. We further analyzed small-world behaviour and local and global efficiency of the subnetworks.

To further demonstrate whether brain regions captured by nodal degree reveal information for both mild and major depression, we performed *t* tests on the degrees of all 90 nodes for the 3 contrasts, controlling for age, sex, years of education, lesion size, MMSE score and NIHSS score. Multiple comparisons were corrected using the FDR method.

Assessment of the unique contribution of identified subnetworks for major depression using Poisson regression with robust standard errors

Given the high prevalence of major depression in poststroke patients, we used Poisson regression with robust standard errors (rather than binary logistic regression) to assess the unique contribution of the identified subnetwork toward the presence of major depression. As the outcome incidence increases, binary logistic regression could be problematic through overestimation of risk ratios, while Poisson regression with robust standard errors has been demonstrated to give correct risk ratios and confidence intervals (CI) in these situations.[34,35] The baseline characteristic variables and the topological properties of brain networks with significance levels of *p* < 0.20 after a univariate analysis were entered into the Poisson regression with robust standard errors.

All statistical assessments were 2-tailed, and we considered results to be significant at *p* < 0.05, consistent with the preliminary status of the trial. We used SPSS 15.0 statistical software (SPSS Inc.) to perform our analyses.

Results

We recruited 135 patients to the study, and 116 met the inclusion criteria. Of the 19 excluded patients, 7 had a history of mental disorders or were taking antidepressants, 2 had a history of dementia, 1 had a history of drug abuse, 5 had severe aphasia that precluded cooperation with the evaluations and clinical interview, and 4 were severe drinkers. Fourteen patients (12.1%) received a diagnosis of major depression, 26 (22.4%) had mild depression, and 76 (65.5%) fell in the control group. Baseline characteristics are shown in Table 1.

Statistical parametric mapping results for lesion areas associated with PSD

The mild depression – control contrast revealed 2 clusters associated with mild depression (Fig. 1, top row; peak MNI coordinates were left thalamus: *x*, *y*, *z* = –12, –16, 6; left putamen: *x*, *y*, *z* = –24, –8, 6). The major depression – control contrast revealed 3 clusters associated with major depression (Fig. 1, middle row; peak MNI coordinates were right insular cortex: *x*, *y*, *z* = 30, 26, 0; left putamen: *x*, *y*, *z* = –22, 4, 0; right superior longitudinal fasciculus: *x*, *y*, *z* = 30, –24, 2). The major depression – mild depression contrast revealed 2 clusters associated more with major depression than with mild depression (Fig. 1, bottom row; peak MNI coordinates were right insular cortex: *x*, *y*, *z* = 30, 26, 0; right superior longitudinal fasciculus: *x*, *y*, *z* = 30, –18, 18). All results were corrected for multiple comparisons.

Whole brain voxel-based FA analysis

We found statistically significant FA reductions in each contrast. Regions revealed by the mild depression – control and major

Table 1: Summary of baseline characteristics of the 116 poststroke patients

	Group, no. (%) or mean ± SD			
Characteristic	Control (*n* = 76)	Mild depression (*n* = 26)	Major depression (*n* = 14)	*p* value*
Age, yr	66.0 ± 10.1	71.2 ± 6.7	71.0 ± 8.0	0.021
Male sex	50 (65.8)	16 (61.5)	10 (71.4)	0.82
Female sex	26 (34.2)	10 (39.5)	4 (29.6)	0.82
Education, yr	8.2 ± 4.4	7.5 ± 4.7	6.1 ± 3.9	0.25
History of drinking				0.28
Nondrinkers	40 (52.6)	9 (34.6)	7 (50.0)	—
Light drinkers	14 (18.4)	6 (23.1)	5 (35.7)	—
Moderate drinkers	15 (19.7)	5 (19.2)	1 (7.1)	—
Ex-drinkers	7 (9.2)	6 (23.1)	1 (7.1)	—
NIHSS score	1.2 ± 1.4	2.1 ± 2.2	1.4 ± 1.5	0.06
MMSE score	26.2 ± 3.8	22.3 ± 5.1	23.1 ± 3.1	< 0.001
BI	75.6 ± 13.8	73.1 ± 21.0	77.9 ± 10.0	0.29

BI = Barthel Index; MMSE = Mini Mental State Examination; NIHSS = National Institutes of Health Stroke Score; SD = standard deviation.
*Independent 1-way analysis of variance and χ² tests.

depression – control contrasts survived FWE correction (Fig. 2, top and middle rows, respectively). The third contrast revealed brain regions with greater FA reductions in patients with major depression than in those with minor depression (Fig. 2, bottom row, $p < 0.001$, uncorrected). The positive clusters for the 3 contrasts are illustrated in the Appendix, Tables S1–S3, available at jpn.ca.

Fractional anisotropy values in intact areas of lesioned tracts

We found that the mean FA of the intact areas within lesioned tracts was lower than with completely intact white matter tracts

$(0.33 \pm 0.14$ v. 0.37 ± 0.23, $p = 0.008)$. The Appendix, Fig. S1, shows the results from 17 identified tracts. Mean FA values of intact voxels in the 17 white matter tracts did not significantly differ between nondrinkers and light to moderate drinkers.

Brain nodes whose degrees were correlated with severity of depression

Intriguingly, 17 nodes showed a significant correlation between nodal degree and HAMD-24 score (Table 2). Five were in the frontal lobe (20 nodes, 25%), 2 in the insula (2 nodes, 100%), 2 in the limbic system (12 nodes, 16.7%), 2 in the parietal lobe
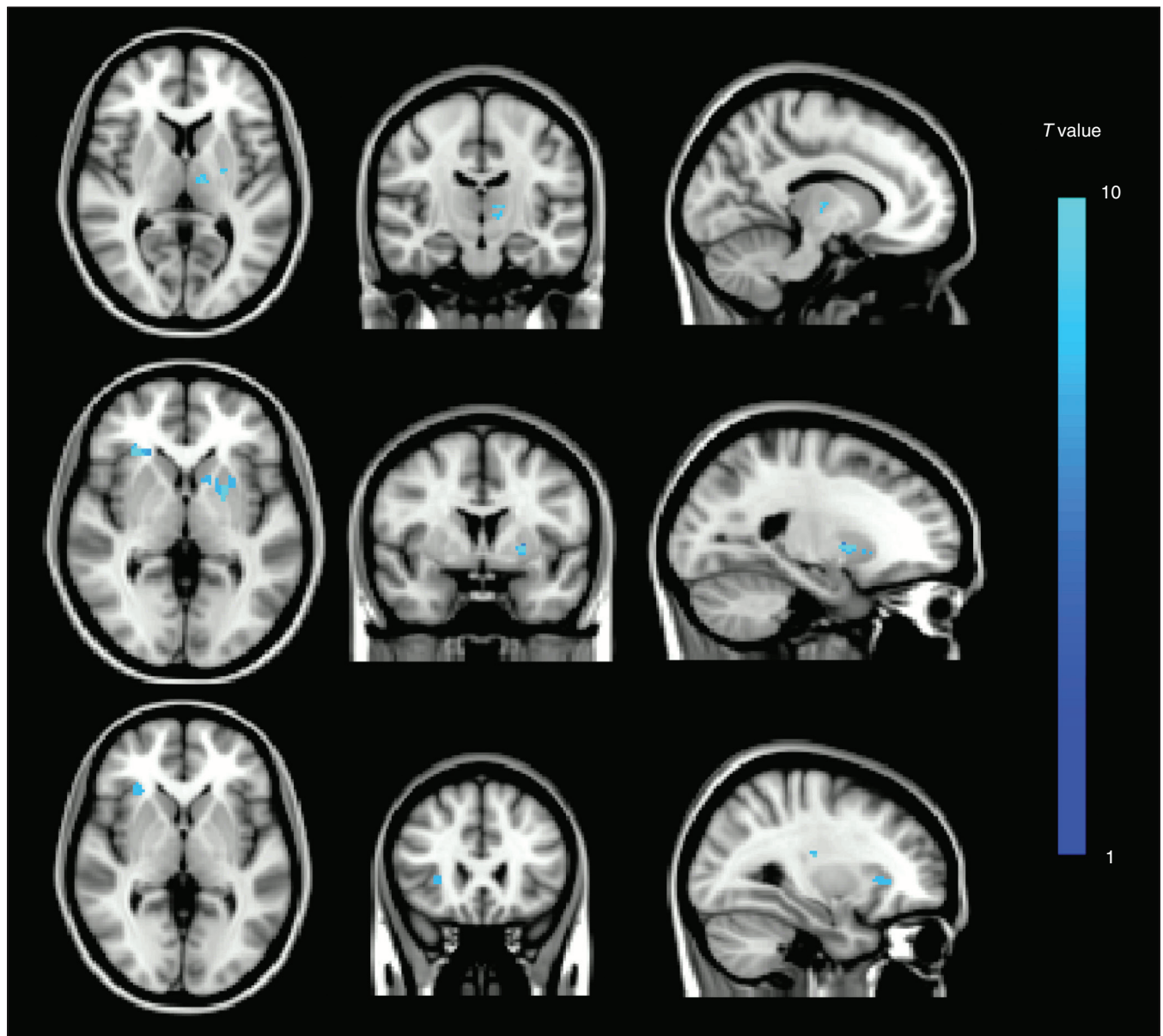
Fig. 1: Overlap of positive brain regions in the whole brain voxel-based lesion analysis using statistical parametric mapping. (**Top**) Mild depression – control contrast. (**Middle**) Major depression – control contrast. (**Bottom**) Major depression – mild depression contrast. All results are family-wise error–corrected for multiple comparisons with cluster sizes > 100 voxels.

(14 nodes, 14.3%), 3 in the basal ganglia area (8 nodes, 37.5%) and 3 in the temporal lobe (12 nodes, 25.0%). The whole brain network could therefore be divided into 2 subnetworks: a depression-related subnetwork composed of 17 nodes (Fig. 3) and a depression-unrelated subnetwork formed by the other 73 nodes.

We compared nodal degrees for the 3 contrasts, and details are shown in the Appendix, Table S4. After correcting for multiple comparisons (FDR method), analysis showed that the same 10 nodes in the depression-related subnetwork were associated with both mild depression and major depression compared with controls. Nine nodes were found to be associated more with major depression than with mild depression, but this finding did not survive FDR correction.

Contribution of the depression-related subnetwork toward major depression

Using graph theoretical analyses, we found that the whole brain white matter networks, the depression-related subnetwork and the depression-unrelated subnetwork showed high σ values (2.96 ± 0.99, 2.13 ± 0.56, and 2.67 ± 0.45, respectively).

Table 3 presents the results of analyses using Poisson regression with robust standard errors that we conducted to determine whether any factors were associated with post-stroke major depression. Analysis indicated that decreased local efficiency in the depression-related subnetwork (relative risk 0.84, 95% CI 0.72–0.98, $p = 0.027$) was a significant risk factor for the presence of major depression after stroke.
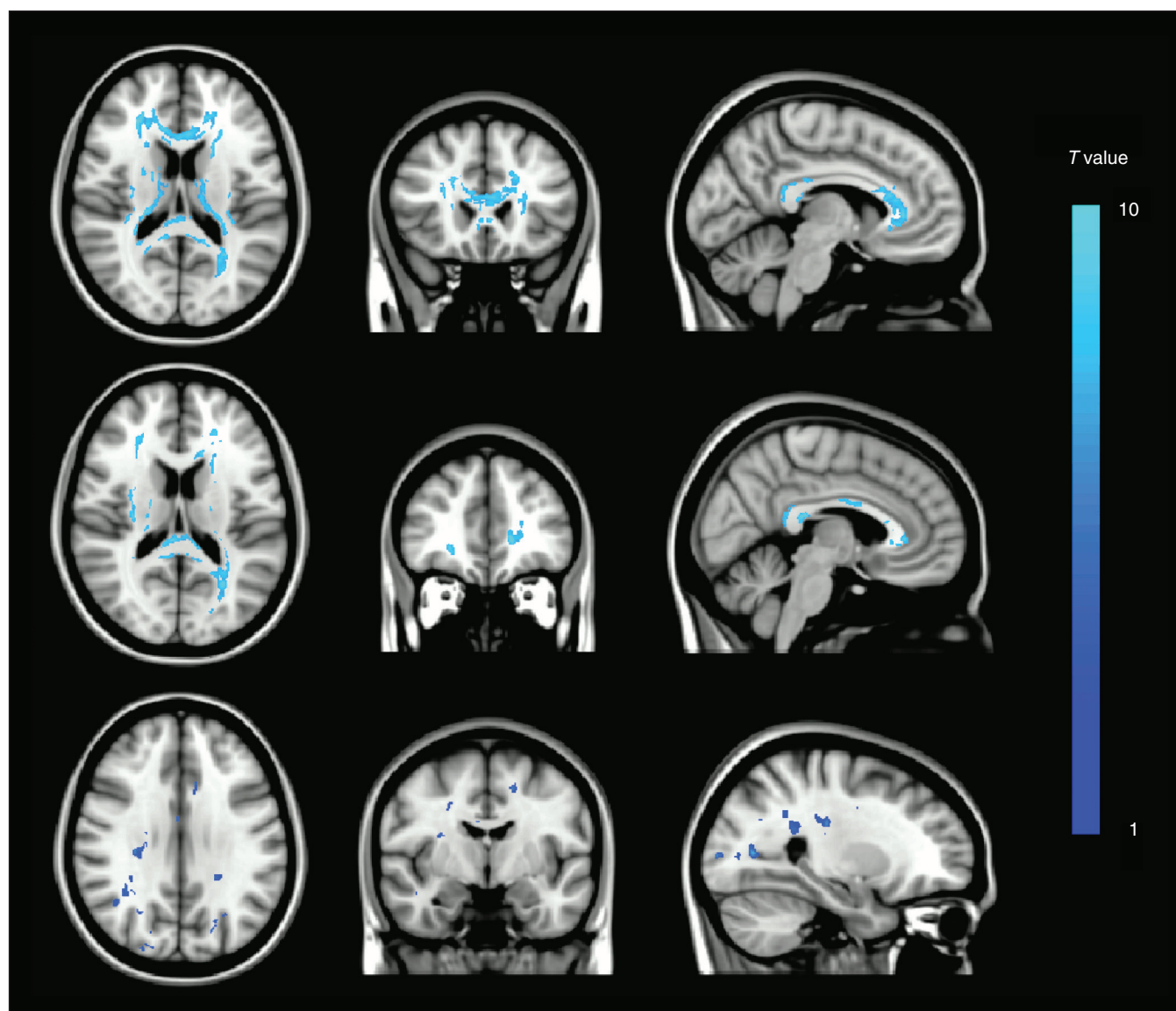
Fig. 2: Overlap of positive brain regions in the whole brain voxel-based fractional anisotropy analysis using statistical parametric mapping. Clusters revealed by the (**Top**) mild depression – control and (**Middle**) major depression – control contrasts survived family-wise error–correction. Clusters revealed by the (**Bottom**) major depression – mild depression contrast are thresholded at $p < 0.001$, uncorrected.

Discussion

Using structural and diffusion MRI data from 116 poststroke patients, we showed that lesions located in the left thalamus and left putamen were associated with mild depression and that lesions in the right insular cortex, left putamen and right superior longitudinal fasciculus were associated with major depression. In addition, FA reduction in broader areas was linked to both mild and major depression. However, the functions that the observed lesions and changes in white matter serve with regards to processing emotions need to be understood in the context of brain connectivity. Therefore, we explored white matter connectivity between 90 brain regions defined by the AAL atlas using graph theory and identified a depression-related subnetwork composed of 17 brain regions.

Our results showing that lesions located in the left thalamus, left putamen, right insular cortex and right superior longitudinal fascicle were associated with PSD are in line with those of previous studies[5,36] and add important evidence supporting the theory that PSD is linked to lesion location during the acute or subacute stroke phase.[5] Our results also showed that decreased mean FA values in broader bilateral areas were associated with PSD. However, what mechanism underlies decreases in FA and how functioning in the presence of PSD is affected are important questions. Fractional anisotropy is a scalar value between zero and 1 that reflects fibre density, axonal diameter and myelination in white matter,[37] and its reduction is a sign of degradation of the microstructural organization in white matter.[38] White matter changes as a consequence of small vessel disease have been linked to late-life depression[39] and have been associated with decreases in FA in specific white matter areas.[37] Lesioned

brain regions have also been shown to have lower FA values than intact regions,[40] and here we demonstrated that intact areas of lesioned tracts also have lower mean FA values than intact tracts. Fractional anisotropy may provide additional information regarding the effects of Wallerian degeneration and other kinds of axonal degeneration after stroke,[41] which may be undetectable using conventional imaging.

After a stroke, the effects on white matter tract integrity caused by the primary lesion can be both local and distal.[42] To understand brain damage in the context of neural connectivity, we performed partial correlations between the degree of a node and the HAMD-24 score to analyze the correlation between brain region connectivity and severity of depression. We chose nodal degree because the number of connections or edges a node has to other nodes has been demonstrated to be a reliable index of network integrity.[43]

We identified 17 brain regions whose nodal degree was negatively correlated with HAMD-24 scores. They included the prefrontal cortex, parietal cortex (right precentral gyrus and left precuneus gyrus), temporal cortex (bilateral fusiform and left superior temporal gyrus), the limbic system (bilateral posterior cingulum) and related brain areas (bilateral insula) and the basal ganglia (bilateral caudate and right putamen). Studies have identified the putamen and insula as parts of a "hate circuit,"[44] while the bilateral precuneus, known as the hub of the default mode network, has been linked to ratings of one's own personality traits.[45] The left superior temporal gyrus has been associated with the perception of emotions in facial stimuli, and abnormalities in this area have been linked to depression.[46] Given that a recent meta-analysis linked major depressive disorder to the white matter fascicles connecting the prefrontal cortex

Table 2: Depression-related brain regions*

| Location	Brain region	Nodal degree	
		r	p value
Frontal lobe (n = 5)	L superior frontal gyrus, dorsolateral	−0.408	0.002
	R superior frontal gyrus, dorsolateral	−0.510	< 0.001
	L inferior frontal gyrus, triangular part	−0.446	< 0.001
	L olfactory cortex	−0.472	< 0.001
	L superior frontal gyrus, medial	−0.438	0.001
Insula (n = 2)	L insula	−0.510	< 0.001
	R insula	−0.455	< 0.001
Limbic system (n = 2)	L posterior cingulate gyrus	−0.452	0.001
	R posterior cingulate gyrus	−0.416	0.002
Parietal lobe (n = 2)	R precentral gyrus	−0.412	0.002
	L precuneus	−0.407	0.002
Basal ganglia (n = 3)	L caudate nucleus	−0.436	0.001
	R caudate nucleus	−0.410	0.002
	R lenticular nucleus, putamen	−0.512	< 0.001
Temporal lobe (n = 3)	L fusiform gyrus	−0.438	0.001
	R fusiform gyrus	−0.424	0.001
	L superior temporal gyrus	−0.430	0.001

L = left; R = right.
*False-discovery rate correction (p < 0.0024, corrected p < 0.05). The full names of the abbreviations are listed in supplemental Table 6.

Table 3: Determinants of significant risk factors associated with major depression using Poisson regression with robust standard errors

Variable	RR (95% CI)	*p* value
Age, yr	0.98 (0.95–1.01)	0.23
Education, yr	0.93 (0.83–1.03)	0.18
MMSE score	1.07 (0.88–1.33)	0.48
Depression-related subnetwork		
Local efficiency	0.84 (0.72–0.98)	0.027
Global efficiency	0.87 (0.75–1.01)	0.06
The depression-unrelated subnetwork		
Local efficiency	1.25 (0.75–2.10)	0.39
Global efficiency	0.50 (0.12–2.08)	0.34
The whole brain network		
Local efficiency	0.85 (0.37–1.96)	0.70
Global efficiency	1.77 (0.33–9.06)	0.51

CI = confidence interval; MMSE = Mini Mental State Examination; RR = relative risk.
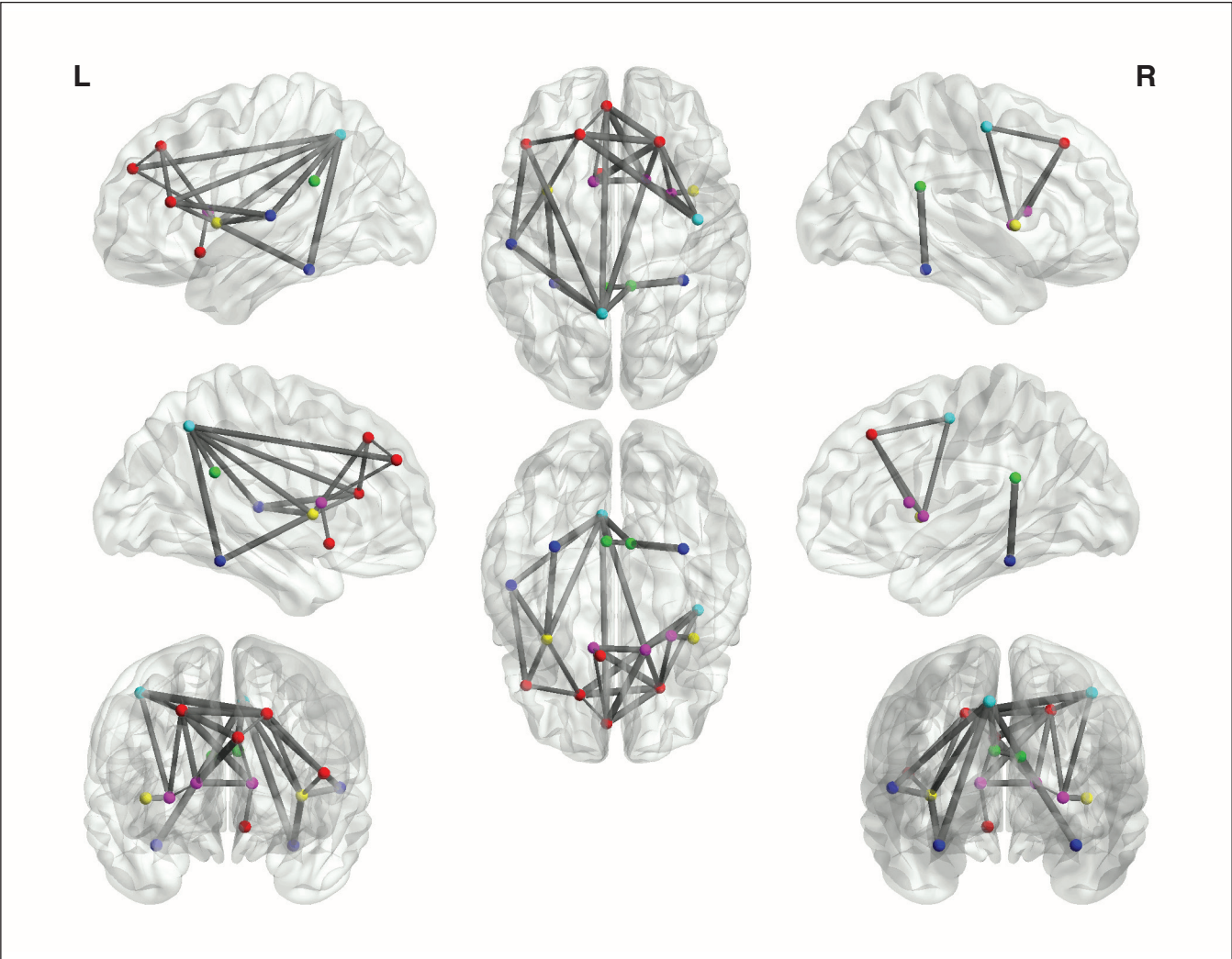
Fig. 3: The depression-related subnetwork. Every ball denotes a brain node and every line denotes a connection. Different coloured nodes represent different brain regions: red = frontal cortex, violet = basal ganglia, blue = parietal cortex, dark blue = temporal cortex, green = limbic system and yellow = insula.

within cortical (frontal, temporal, and occipital lobes) and subcortical areas (amygdala and hippocampus) by voxel-based analysis of DTI studies,[47] our results provide evidence for the presence of PSD, indicating that structural damage to emotion-related networks leads to depressive syndromes after stroke.

However, as part of the depression-related subnetwork, the bilateral posterior cingulate, prefrontal cortex, basal ganglia and related brain regions are also linked to memory, executive function and mediation between emotion and memory.[48] Damage to this subnetwork might cause deterioration of cognitive function. Given that a high prevalence of cognitive impairment has been reported in PSD,[49] our results are in line with this and provide a structural basis.

Our results also showed that decreased local efficiency of the depression-related subnetwork was linked to poststroke major depression. Given that high local efficiency reflects an optimal status in local communication,[29,50] our findings suggest that patients with poststroke major depression exhibit less efficient topological organization in their white matter networks. Decreased local efficiency caused by structural damage can make the network less fault tolerant; that is, damage or disconnection of one brain region in the network will dramatically affect the connection between its previously linked regions.[29] This pattern has been reported in other neurologic conditions, such as Alzheimer disease.[51] Global efficiency, which is primarily associated with effective or rapid information transfers between remote brain regions,[52] didn't survive the Poisson regression. Because structural connections in the human brain have evolved into a complex and efficient neuronal network,[52] compensation for damage likely occurs over broad regions.

Limitations

The first of our study's limitations is that the DTI deterministic tractography used to reconstruct the whole brain networks has been shown to have a limited capacity for resolving crossing fibre bundles.[24] This might affect our PSD-related findings. Probabilistic diffusion tractography[53] is a promising technique that might yield more accurate brain networks in future studies. Second, to understand regional changes in the context of brain connectivity, we explored brain structural network using graph theory. However, it would be more intriguing in the future to construct an integrated approach relating regional brain damage to the depression-related network. Third, the diagnosis of depression itself was relatively weak, as it was made on clinical grounds by a neuropsychologist. The Structured Clinical Interview for DSM disorders should be used in future study. Finally, the HAMD-24 score was used to identify the nodes as being part of the depression-related network, and then this network was used to predict PSD. Therefore, the association between depression and efficiency of the depression-related network needs to be replicated in the future.

Conclusion

The present study provides, to our knowledge, the first graph theoretical analysis of white matter networks linked to PSD. We identified a depression-related subnetwork composed of 17 brain regions. We found that decreased local efficiency of the depression-related subnetwork was a significant risk factor for the presence of poststroke major depression. These findings provide new insights into the neuroanatomical substrates of PSD.

Affiliations: From the Department of Experimental Psychology, University of Oxford, Oxford, United Kingdom (Yang, Humphreys); the Department of Cardiovascular Surgery, Sun Yat-sen Memorial Hospital, Sun Yat-sen University, Guangzhou, China (Hua); the Department of Neurology, Guangzhou First People's Hospital, Guangzhou Medical University, Guangzhou, China (Shang); and the State Key Laboratory of Cognitive Neuroscience and Learning, Beijing Normal University, Beijing, China (Cui, Zhong, Gong).

Competing interests: None declared.

Contributors: S. Yang, P. Hua and G. Gong designed the study. S. Yang, P. Hua, X. Shang, Z. Cui and S. Zhong acquired and analyzed the data, which G. Humphreys also analyzed. S. Yang, P. Hua, X. Shang, Z. Cui and S. Zhong wrote the article, which all authors reviewed and approved for publication.

References

1. Meader N, Moe-Byrne T, Llewellyn A, et al. Screening for poststroke major depression: a meta-analysis of diagnostic validity studies. *J Neurol Neurosurg Psychiatry* 2014;85:198-206.

2. Hornsten C, Lovheim H, Gustafson Y. The association between stroke, depression, and 5-year mortality among very old people. *Stroke* 2013;44:2587-9.

3. Drevets WC, Price JL, Furey ML. Brain structural and functional abnormalities in mood disorders: implications for neurocircuitry models of depression. *Brain Struct Funct* 2008;213:93-118.

4. Carson AJ, MacHale S, Allen K, et al. Depression after stroke and lesion location: a systematic review. *Lancet* 2000;356:122-6.

5. Murakami T, Hama S, Yamashita H, et al. Neuroanatomic pathways associated with poststroke affective and apathetic depression. *Am J Geriatr Psychiatry* 2013;21:840-7.

6. Bhogal SK, Teasell R, Foley N, et al. Lesion location and poststroke depression: systematic review of the methodological limitations in the literature. *Stroke* 2004;35:794-802.

7. Bullmore ET, Bassett DS. Brain graphs: graphical models of the human brain connectome. *Annu Rev Clin Psychol* 2011;7:113-40.

8. Bullmore E, Sporns O. Complex brain networks: graph theoretical analysis of structural and functional systems. *Nat Rev Neurosci* 2009;10:186-98.

9. Bai F, Shu N, Yuan Y, et al. Topologically convergent and divergent structural connectivity patterns between patients with remitted geriatric depression and amnestic mild cognitive impairment. *J Neurosci* 2012;32:4307-18.

10. Shu N, Liu Y, Li J, et al. Altered anatomical network in early blindness revealed by diffusion tensor tractography. *PLoS ONE* 2009;4:e7228.

11. Brown JA, Terashima KH, Burggren AC, et al. Brain network local interconnectivity loss in aging APOE-4 allele carriers. *Proc Natl Acad Sci U S A* 2011;108:20760-5.

12. Crofts JJ, Higham DJ, Bosnell R, et al. Network analysis detects changes in the contralesional hemisphere following stroke. *Neuroimage* 2011;54:161-9.

13. Wannamethee SG, Shaper AG. Lifelong teetotallers, ex-drinkers and drinkers: mortality and the incidence of major coronary heart disease events in middle-aged British men. *Int J Epidemiol* 1997;26:523-31.

14. Bagga D, Sharma A, Kumari A, et al. Decreased white matter integrity in fronto-occipital fasciculus bundles: relation to visual information processing in alcohol-dependent subjects. *Alcohol* 2014;48:43-53.

15. Yang SR, Hua P, Shang XY, et al. Predictors of early post ischemic stroke apathy and depression: a cross-sectional study. *BMC Psychiatry* 2013;13:164.

16. Hamilton M. Development of a rating scale for primary depressive illness. *Br J Soc Clin Psychol* 1967;6:278-96.

17. Jenkinson M, Smith S. A global optimisation method for robust affine registration of brain images. *Med Image Anal* 2001;5:143-56.

18. Altieri M, Maestrini I, Mercurio A, et al. Depression after minor stroke: prevalence and predictors. *Eur J Neurol* 2012;19:517-21.

19. Nys GM, van Zandvoort MJ, van der Worp HB, et al. Early depressive symptoms after stroke: neuropsychological correlates and lesion characteristics. *J Neurol Sci* 2005;228:27-33.

20. Hua K, Zhang J, Wakana S, et al. Tract probability maps in stereotaxic spaces: analyses of white matter anatomy and tract-specific quantification. *Neuroimage* 2008;39:336-47.

21. Cui Z, Zhong S, Xu P, et al. PANDA: a pipeline toolbox for analyzing brain diffusion images. *Front Hum Neurosci* 2013;7:42.

22. Gong G, He Y, Concha L, et al. Mapping anatomical connectivity patterns of human cerebral cortex using in vivo diffusion tensor imaging tractography. *Cereb Cortex* 2009;19:524-36.

23. Tzourio-Mazoyer N, Landeau B, Papathanassiou D, et al. Automated anatomical labeling of activations in SPM using a macroscopic anatomical parcellation of the MNI MRI single-subject brain. *Neuroimage* 2002;15:273-89.

24. Mori S, van Zijl PC. Fiber tracking: principles and strategies — a technical review. *NMR Biomed* 2002;15:468-80.

25. Mori S, Crain BJ, Chacko VP, et al. Three-dimensional tracking of axonal projections in the brain by magnetic resonance imaging. *Ann Neurol* 1999;45:265-9.

26. Wen W, Zhu W, He Y, et al. Discrete neuroanatomical networks are associated with specific cognitive abilities in old age. *J Neurosci* 2011;31:1204-12.

27. van den Heuvel MP, Kahn RS, Goni J, et al. High-cost, high-capacity backbone for global brain communication. *Proc Natl Acad Sci U S A* 2012;109:11372-7.

28. He Y, Chen Z, Evans A. Structural insights into aberrant topological patterns of large-scale cortical networks in Alzheimer's disease. *J Neurosci* 2008;28:4756-66.

29. Latora V, Marchiori M. Efficient behavior of small-world networks. *Phys Rev Lett* 2001;87:198701.

30. Shu N, Liu Y, Li K, et al. Diffusion tensor tractography reveals disrupted topological efficiency in white matter structural networks in multiple sclerosis. *Cereb Cortex* 2011;21:2565-77.

31. Achard S, Bullmore E. Efficiency and cost of economical brain functional networks. *PLOS Comput Biol* 2007;3:e17.

32. Humphries MD, Gurney K, Prescott TJ. The brainstem reticular formation is a small-world, not scale-free, network. *Proc Biol Sci* 2006;273:503-11.

33. Achard S, Salvador R, Whitcher B, et al. A resilient, low-frequency, small-world human brain functional network with highly connected association cortical hubs. *J Neurosci* 2006;26:63-72.

34. Knol MJ, Le Cessie S, Algra A, et al. Overestimation of risk ratios by odds ratios in trials and cohort studies: alternatives to logistic regression. *CMAJ* 2012;184:895-9.

35. Zou G. A modified poisson regression approach to prospective studies with binary data. *Am J Epidemiol* 2004;159:702-6.

36. Paradiso S, Ostedgaard K, Vaidya J, et al. Emotional blunting following left basal ganglia stroke: the role of depression and fronto-limbic functional alterations. *Psychiatry Res* 2013;211:148-59.

37. Soriano-Raya JJ, Miralbell J, Lopez-Cancio E, et al. Tract-specific fractional anisotropy predicts cognitive outcome in a community sample of middle-aged participants with white matter lesions. *J Cereb Blood Flow Metab* 2014;34:861-9.

38. van der Holst HM, Tuladhar AM, van Norden AG, et al. Microstructural integrity of the cingulum is related to verbal memory performance in elderly with cerebral small vessel disease: the RUN DMC study. *Neuroimage* 2013;65:416-23.

39. Teodorczuk A, Firbank MJ, Pantoni L, et al. Relationship between baseline white-matter changes and development of late-life depressive symptoms: 3-year results from the LADrosoph Inf Serv study. *Psychol Med* 2010;40:603-10.

40. Kim J, Lee SK, Lee JD, et al. Decreased fractional anisotropy of middle cerebellar peduncle in crossed cerebellar diaschisis: diffusion-tensor imaging-positron-emission tomography correlation study. *AJNR Am J Neuroradiol* 2005;26:2224-8.

41. Yu C, Zhu C, Zhang Y, et al. A longitudinal diffusion tensor imaging study on Wallerian degeneration of corticospinal tract after motor pathway stroke. *Neuroimage* 2009;47:451-8.

42. Liang Z, Zeng J, Liu S, et al. A prospective study of secondary degeneration following subcortical infarction using diffusion tensor imaging. *J Neurol Neurosurg Psychiatry* 2007;78:581-6.

43. Wang JH, Zuo XN, Gohel S, et al. Graph theoretical analysis of functional brain networks: test-retest evaluation on short- and long-term resting-state functional MRI data. *PLoS ONE* 2011;6:e21976.

44. Zeki S, Romaya JP. Neural correlates of hate. *PLoS ONE* 2008;3:e3556.

45. Lou HC, Luber B, Crupain M, et al. Parietal cortex and representation of the mental Self. *Proc Natl Acad Sci U S A* 2004;101:6827-32.

46. Liu F, Hu M, Wang S, et al. Abnormal regional spontaneous neural activity in first-episode, treatment-naive patients with late-life depression: a resting-state fMRI study. *Prog Neuropsychopharmacol Biol Psychiatry* 2012;39:326-31.

47. Liao Y, Huang X, Wu Q, et al. Is depression a disconnection syndrome? Meta-analysis of diffusion tensor imaging studies in patients with MDD. *J Psychiatry Neurosci* 2013;38:49-56.

48. Maddock RJ, Garrett AS, Buonocore MH. Posterior cingulate cortex activation by emotional words: fMRI evidence from a valence decision task. *Hum Brain Mapp* 2003;18:30-41.

49. Ayerbe L, Ayis S, Wolfe CD, et al. Natural history, predictors and outcomes of depression after stroke: systematic review and meta-analysis. *Br J Psychiatry* 2013;202:14-21.

50. Sporns O, Tononi G, Edelman GM. Theoretical neuroanatomy: relating anatomical and functional connectivity in graphs and cortical connection matrices. *Cereb Cortex* 2000;10:127-41.

51. Reijmer YD, Leemans A, Caeyenberghs K, et al. Disruption of cerebral networks and cognitive impairment in Alzheimer disease. *Neurology* 2013;80:1370-7.

52. He Y, Dagher A, Chen Z, et al. Impaired small-world efficiency in structural cortical networks in multiple sclerosis associated with white matter lesion load. *Brain* 2009;132:3366-79.

53. Behrens TE, Berg HJ, Jbabdi S, et al. Probabilistic diffusion tractography with multiple fibre orientations: What can we gain? *Neuroimage* 2007;34:144-55.